



# STRESS

## IN DIAMOND-COATED CUTTING TOOLS

Diamond coatings make cutting tools more effective, but only if the layer remains intact. Read on to learn about how machining stress can lead to delamination, and failure.

By Jianwen Hu, Y. Kevin Chou, and Raymond G. Thompson

**D**iamond coatings have been increasingly used in cutting-tool applications. Coating delamination is the major tool failure mode and occurs due to deposition-induced residual stresses and thermo-mechanical loading in machining. This study applies finite element analysis to investigate stress distributions—with a focus on the edge radius—in diamond coating tools considering depositions and machining.

After depositions the residual stresses around the edge are compressive and tensile for the radial and tangential components, respectively, with high stress concentrations. The stress concentrations can be alleviated by a large edge radius. When machining loading is imposed, stress reversal occurs on both components, i.e., radial (or tangential) stresses shifting toward less tensile (or compressive). For the edge radius effects, at a low feed, increasing the hone radius will reduce the maximum tangential normal stress (from compression toward tension). However, the edge radius seems to have minor effects at a high feed.

## Introduction

Diamond is the ideal candidate to machine non-ferrous materials because of its high hardness/strength, low friction coefficient, and chemical stability, etc. Diamond turning of ultra-precision components, e.g. mirror-finish optics, requires single-crystal gem-quality nature diamond. Synthetic polycrystalline diamond (PCD), made by high-pressure high-temperature sintering, is more commonly used in the manufacturing industry. However, processing and fabrications of PCD tools are of high cost, too. On the other hand, diamond coatings using advanced surface engineering technologies such as chemical vapor deposition (CVD) have been increasingly explored for cutting-tool applications. Diamond coated tools have great potential in various machining applications and an advantage in the fabrication of cutting tools with complex geometry such as drills. Increased usages of lightweight high-strength components have

also resulted in significant interests in diamond coating tools.

Hot-filament CVD is the primary process of diamond coatings because of the relative low cost of equipment and mature fabrication technologies. Thin film CVD diamond over 50  $\mu\text{m}$  thick has been deposited on various materials including tungsten carbide. Applications of CVD diamond coating tools have been frequently reported. It is the consensus that CVD diamond tools generate poor surface finish compared to PCD due to rough coating surfaces. Though post-deposition polishing of the coating may improve part surface finish (Arumugam et al., 2006), the additional step is expensive and difficult to perform on complex shapes. On tool life, however, there are mixed results of CVD diamond performance. In a few applications CVD diamond shows greater wear resistance than PCD tools. Oles et al. applied different treatments to enhance diamond coating adhesion (Oles et al., 1996). In machining testing of high-Si Al alloys the results show that CVD diamond tools can meet or even exceed PCD in tool life. Shen also tested CVD diamond tools from a variety of sources and reported that some coatings have performance comparable to PCD, but cited large variations of coating performance (Shen, 1994 and 1996). On the other hand, there are several studies showing that the tool wear resistance of CVD diamond is still inferior to PCD (Karner et al., 1996, Schafer et al., 1999, D'Errico and Calzavarini, 2001, Davim, 2002, Polini et al., 2003, etc.). For example, D'Errico and Calzavarini tested CVD diamond tools from different manufacturers against PCD in machining Al-based composite. It was concluded that CVD diamond tools have shorter tool lives than PCD, though CVD diamond may have potential

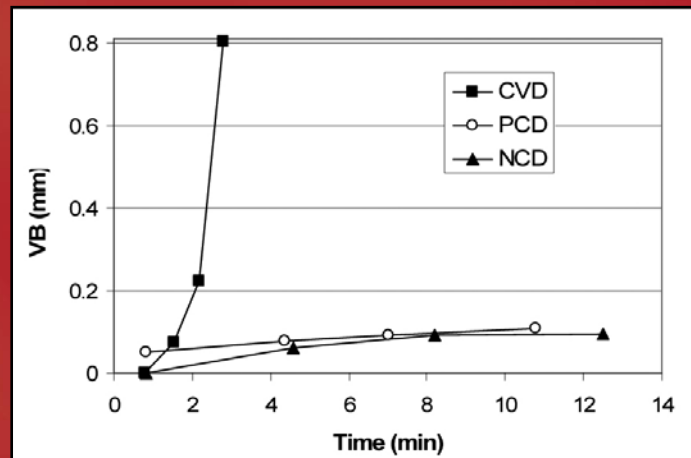
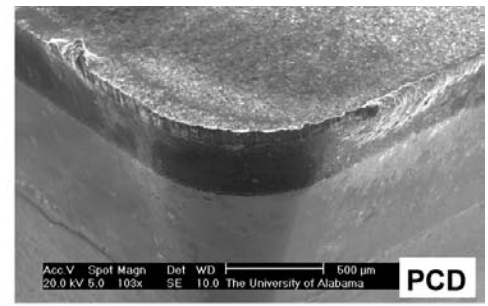
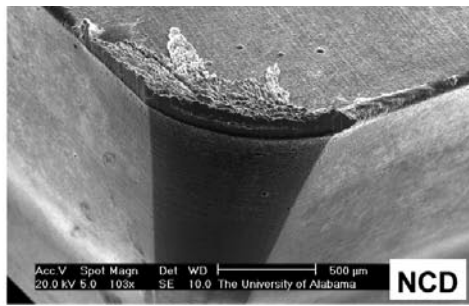
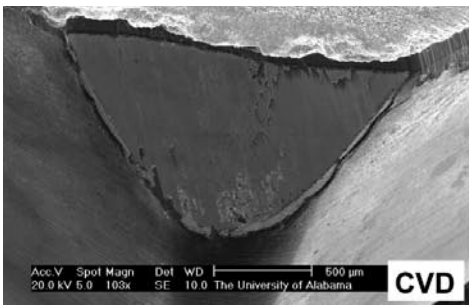


FIGURE 1: TOOL FLANK WEAR VS. TIME



**FIGURE 2: DIAMOND TOOL WEAR AFTER COMPOSITE MACHINING**

economical benefit because of multiple edges. The authors further examined the coating failure zone by scanning electron microscopy (SEM) and observed coating flaking and gaps between the coating and the substrate, also reported by others. Our previous work also demonstrated that coating delamination at the tool flank can be of a catastrophic nature and is the tool-life limiting factor for CVD diamond tools (Chou and Liu, 2005). High stresses and/or degraded adhesion during machining result in coating failure and the exposed substrate suffers from massive deformation and rapid wear.

Recently a microwave-plasma CVD technology has been developed to increase the diamond growth rate and, with nitrogen

gas, to produce fine diamond grains on the order of 10 nm (Catledge and Vohra, 1995). The produced nano-structured coatings, which consist of nanocrystals of diamond embedded into a hard amorphous diamond-like carbon matrix, have high hardness and low surface roughness. The newly developed nanocrystalline diamond (NCD) tools were characterized together with CVD diamond and PCD (Hu et al., 2006). Measured surface roughness of the tool rake is listed in Table 1. The CVD diamond has the roughest topography due to the multiple facets of diamond grains. The PCD insert has the smoothest surface from polishing. NCD shows a fairly smooth surface that replicates the texture of the substrate. Nanoindentation testing also

shows that NCD diamond has the highest hardness, followed by CVD and PCD (Table 1).

The three types of diamond tools were further tested in machining Al composite bars to compare their performance. Machining conditions were 4 m/s, 0.05 mm/rev, and 1 mm depth of cut. Part surface finishes produced by the diamond tools prior to failure are also compared in Table 1, rough from CVD diamond and PCD, and better finish by NCD. Figure 1 plots tool wear developments of the diamond tools, and figure 2 shows worn diamond tools after the machining test. CVD diamond had coating failure at short cutting time. The PCD tool reached about 0.11 mm wear-land width after about 10

# Turning Spline Hobbing Into a MILLING OPERATION!

TMFM, LLC introduces their indexable carbide involute spline form milling solution to industry. Utilizing custom ground form inserts and standard, precision ground bodies with a precise insert locking and locating system, TMFM, LLC can turn hobbing operations into a true milling application!



**Spline, Form &  
Special Milling Tools**

AN ADVENT TOOL & MFG AFFILIATE

35 Baker Road • Lake Bluff, IL 60044

877.SPLINE5 • fax 866.267.9950

email: applications@tmfmlc.com • www.tmfmlc.com



*Drop us a line and see what we can do for your application!*

	CVD	NCD	PCD
$R_a^1$ ( $\mu\text{m}$ )	0.47	0.33	0.08
H (GPa)	42 - 66	65 - 93	43 - 53
$R_a^2$ ( $\mu\text{m}$ )	0.60-1.01	0.46-0.75	0.71-1.05

<sup>1</sup>: tool rake face, <sup>2</sup>: machined surface

TABLE 1: CHARACTERISTICS OF DIAMOND TOOLS

min. cutting. For the NCD tools, low wear, comparable to PCD, with some deposits were observed. If the deposit was cleaned (at 8 min. cutting), the tool continued cutting with little noticeable wear increases. Note, however, that if the deposit was not removed, catastrophic delamination occurred, e.g., at 10 min. cutting time and around 0.1 mm VB.

Coating delamination is a major issue in CVD diamond coating (Amirhaghi et al., 2001). Strong adhesion between the coating and the substrate is a key factor to coating performance. With tungsten-carbide (WC) substrates, various techniques have been developed to enhance the adhesion strength (Mallika and Komanduri, 1999). Moreover, largely mismatched thermal expansion coefficients between diamond and WC cause very high stresses in the coating tool and stress discontinuity at the interface. Diamond coating, with a smaller thermal expansion coefficient, is subject to a compressive residual stress, but the carbide substrate in tension. Using literature data: 2.5 and 5.5  $\mu\text{m}/(\text{m}\cdot\text{K})$  of thermal expansion coefficients for CVD diamond and WC, and 1200 GPa and 0.07 for elasticity and Poisson's

ratio of diamond, respectively, a deposition temperature of 800° C can generate a nominal stress in the coating as high as 3.0 GPa in compression. Such high residual stresses will have a compound impact to the coating performance.

The deposition stress estimated above is for the nominal biaxial stress condition. Around any geometric changes, stress distributions will be altered. Using numerical analysis, Gunnars and Alahelsten reported that residual stresses around the substrate edge increase significantly compared to the uniform coating area and small edge radii will drastically increase stress concentrations (Gunnars and Alahelsten, 1996). For machining applications, such high stresses around the cutting edge are obviously crucial because the cutting tip is further subject to localized thermal and mechanical loads. Literature of edge effects on coating tool performance is rather rare. Almeida et al. experimentally studied edge preparations of a diamond coated tool in machining WC (Almeida et al., 2005). Three types of edge conditions—i.e. up-sharp, chamfer, and hone—were tested. The authors indicated that the edge conditions of coating tools significantly affect machining forces, wear pattern, and tool life, etc. It was also shown that coating delamination occurs first at the honed tool, which has a large edge radius, despite possibly reduced stress concentrations.

It is not clear how the cutting edge geometry affects the coating tool performance. To effectively use diamond-coating tools it is necessary to understand the stress modifications around the tool tip due to depositions and machining. By applying finite element analysis (FEA) the goal of this study was to evaluate stress evolutions, affected by the cutting edge, in coating depositions



# BUTLER GEAR

Specializing in Industrial Gear Manufacturing since 1960.

Featuring

- External maag cut gears to 118" diameter
- Internal gears 48" - 12" face
- Spline shaft hob lengths up to 168"
- American and Metric

*"Butler Gear is committed to continuous improvement in technology - to service our customer's needs."*

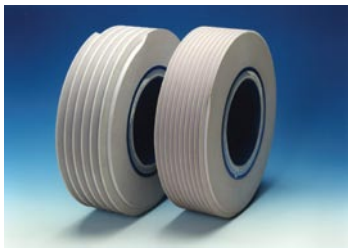
Visit us at [www.butlergear.com](http://www.butlergear.com)  
 Contact us at 12819 Silver Spring Rd Butler, WI 53007  
 Telephone: (262) 781-3270 Fax: (262) 781-1896  
[gears@butlergear.com](mailto:gears@butlergear.com)



ISO 9001 REGISTERED

## Technical Solutions


### Aerospace and Automotive Applications



#### Multiple Start Gear Grinding Wheels

- Lower grinding forces
- New abrasive blends & bonds
- Lower grinding temperatures
- Increased porosity for higher stock removal



#### Gear Honing Benefits



- Flank correction
- Reduced operating noise
- Longer service life
- Correction for distortion from hardening process

**Hermes Abrasives, Ltd.**  
 524 Viking Drive - Virginia Beach, VA 23452  
 PO Box 2389 - Virginia Beach, VA 23450

Toll free phone: 800.464.8314  
 Toll free fax: 800.243.7637

and subsequent machining. Effects of the edge radius and machining parameters on the stress distributions were quantified numerically.

## Stress Analysis

In all simulations the diamond coating tools were modeled with 2D geometry. The substrate, WC, was 12.7 mm wide and 3.18 mm thick, and had an 11° relief angle with different edge geometries. Three edge conditions—namely sharp (edge radius,  $r_e=20\ \mu\text{m}$ ), chamfered ( $20^\circ$  by 2 mm,  $20\ \mu\text{m}\ r_e$ ), and honed ( $r_e=60\ \mu\text{m}$ ,  $100\ \mu\text{m}$ )—were first evaluated in the deposition stress simulation. The diamond coating in the simulation was 30  $\mu\text{m}$  thick as the experimental tools, uniform at the rake and variable thickness at the relief face, linearly decreasing to 0 at about 0.9 mm from the substrate bottom. ANSYS software was used for thermal and mechanical analysis simulations with the plane strain condition assumed. The element geometry chosen had three edges and eight nodes, with dual attributes of Plane77 and Plane82 for thermal and structural analyses, respectively. Meshing

was generated in the coating first using the default setting, and the edge area was refined to about 1.5  $\mu\text{m}$  of element sizes. The substrate was meshed using the default setting.

In deposition-stress simulations, static structural analysis with thermal strains considered was conducted. A deposition temperature of 800° C was set as the initial condition and a room temperature of 25° C as the final temperature. Since both diamond and WC have high melting points and have limited plastic deformation, linear-elastic material models independent of temperatures were used. The elasticity, Poisson's ratio, and thermal expansion coefficient of diamond (Amirhaghi et al., 2001) and WC (Heath, 1986) used were 1200 GPa, 0.07, 2.5  $\mu\text{m}/(\text{m}\cdot\text{K})$ , and 620 GPa, 0.22, 5.5  $\mu\text{m}/(\text{m}\cdot\text{K})$ , respectively. Geometric boundary conditions used in the mechanical analysis were fixed constraints at the two corners. As no efficient 3D FEA machining model with coating stresses considered available, the 2D model from the deposition stress study was carried into the machining simulation. To simulate stress distributions during machining, first transient heat conduction was conducted

to obtain the temperature distributions in the diamond coating tool. The heat flux at the tool-rake contact was estimated using data collected and analyzed from the machining test (Liu and Chou, 2005). The substrate bottom was approximated as the room temperature and other surfaces adiabatic. Temperature-dependent thermal conductivities and constant specific heat and density for both diamond and WC were used (Liu and Chou, 2005). Next a static structural analysis was continued, carrying final temperatures from the thermal analysis and initial stresses from the deposition simulations. The machining-induced contact stresses at the rake face were applied as the mechanical boundary conditions. To estimate the machining loading input to numerical simulations, a set of machining tests was conducted using NCD tools to turn A390 bars with a two-speed (3 ms/ and 10 m/s), two-feed (0.2 mm/rev and 0.8 mm/rev) combination. The depth of cut was 1.0 mm in all cases and the machining time was about 12 seconds, also used in the thermal simulation. Cutting forces were monitored during machining, cutting chips were collected and thickness measured, and the chip-tool

## Yesterday's Reliability Tomorrow's Technology



Fifty years of VARI-ROLL applications provide:

- Production Composite Inspection
- Custom Design & Build Part Gear Mounting Fixtures
- Standard Mounting Fixtures — Spurs, Helicals, Pinion Shafts, Worms, Throated Worms, Bevels, Internals

When coupled with the VARI-PC Composite Gear Analysis System will provide:

- Reduced Inspection Cost
- Improved Accuracy
- Historical Record Keeping
- Serialization of Parts
- Interface to SPC programs

Experience the difference. See why customers worldwide have chosen the VARI-ROLL/VARI-PC. For further information, please contact us.



### VARI-ROLL

**Precision Gage Co., Inc.**  
100 Shore Drive Burr Ridge, IL 60527  
630-653-2121 Fax 630-655-3073  
www.precisiongageco.com



# RPI Repair Parts, Inc.

2415 Kishwaukee St. - Rockford, IL 61104

## WE SPECIALIZE IN:

**Barber-Colman Gear Cutting and  
Hob Sharpening Equipment  
Used, Reconditioned or Rebuilt**

### OEM

Atlantic Van Norman Mills  
• Atlantic Jig Borer

### Services

**Hob & Shaper Cutter Resharpener  
Barber-Colman Hobbing &  
Hob Sharpening Machinery  
Sunstrand Mills, Lathes and Omnimills**



Phone: 815-968-4499  
Fax: 815-968-4694

email: [rpi@repair-parts-inc.com](mailto:rpi@repair-parts-inc.com)  
[www.repair-parts-inc.com](http://www.repair-parts-inc.com)



contact length was measured too. The data was compiled for cutting analysis, orthogonal cutting approximation, to estimate the heat flux and heat partitioning, as well as the normal and shear stresses (all assumed uniform) at the tool rake face (Tables A1 and A2 in appendix). For the edge radius effect on machining forces it is assumed that at a high feed, 0.8 mm/rev, the size effect can be neglected. However, at a low feed, 0.2 mm/rev, the forces—mainly the thrust component—will be changed by edge honing. As there is no data currently available, a linear relationship between force increments and edge-radius increments was assumed, and a proportional constant of 0.25 was estimated (Thiele and Melkote, 1999). Edge radius effects on cutting chip thickness, contact length, and heat partitioning were further considered negligible. The approximated machining forces were then used to evaluate mechanical contact stresses and heat-flux boundary conditions, further implemented into the FEA model. The stress evolution and final stress distributions and maximum value around the tool edge at different machining conditions and different edge radii were evaluated.

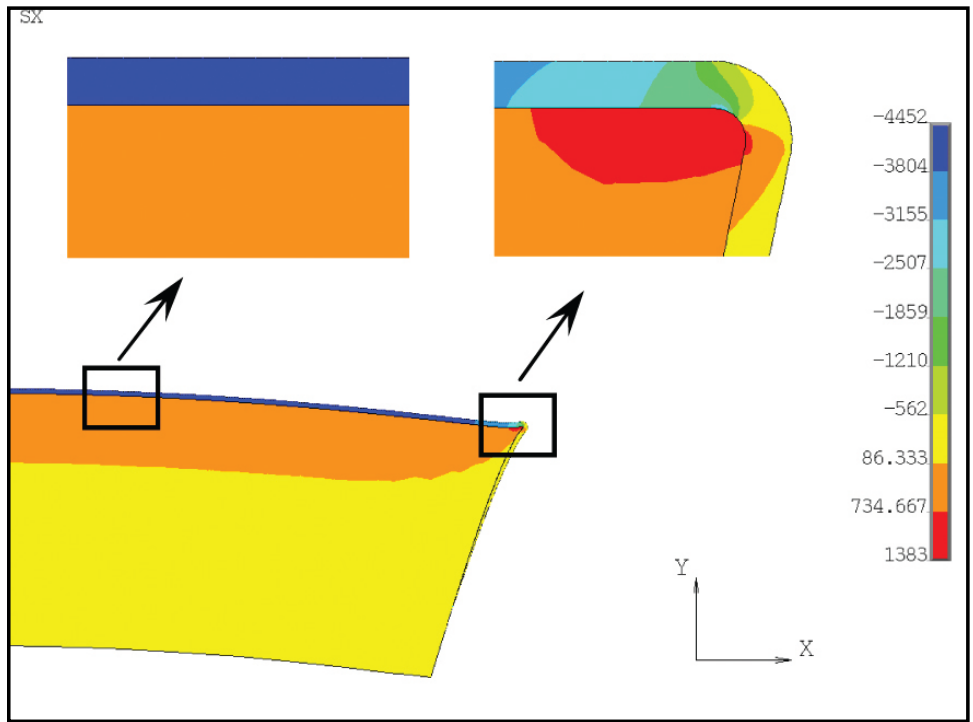


FIGURE 3: AN EXAMPLE OF DEPOSITION STRESS DISTRIBUTIONS

## Results and Discussion

Figure 3 shows typical stress contours (normal component, parallel to the coating surface) after the deposition. The

area away from the edge has a uniform compressive stress around 4.0 GPa in the coating and 0.7 GPa of tension in the substrate. Around the edge, the stress distributions, both values and pattern,

**Gear Hobs  
Gear Shaper Cutters  
Broaching Tools...**

Because our company works closely with several well-established gear tool manufacturers, we can offer **very competitive prices** on stock tools, as well as any special cutters.

**Modern Gearing** Specializes in the sale of Gear Cutting Tools & other Gear-Related Products

Contact us today for a prompt price quote on any special orders, materials and coatings you may require.

**Modern Gearing**

Toll Free:  
Tel: 1-888-595-9897 / Fax: 1-888-595-9860  
www.moderngearing.com

THEM

US

With 8 Billion Encoder Solutions

**Encoder.com**  
Has One Just Right for You!

**Encoder Products Co.**

"For World Class Performance"

© 2002 Encoder Products Co.

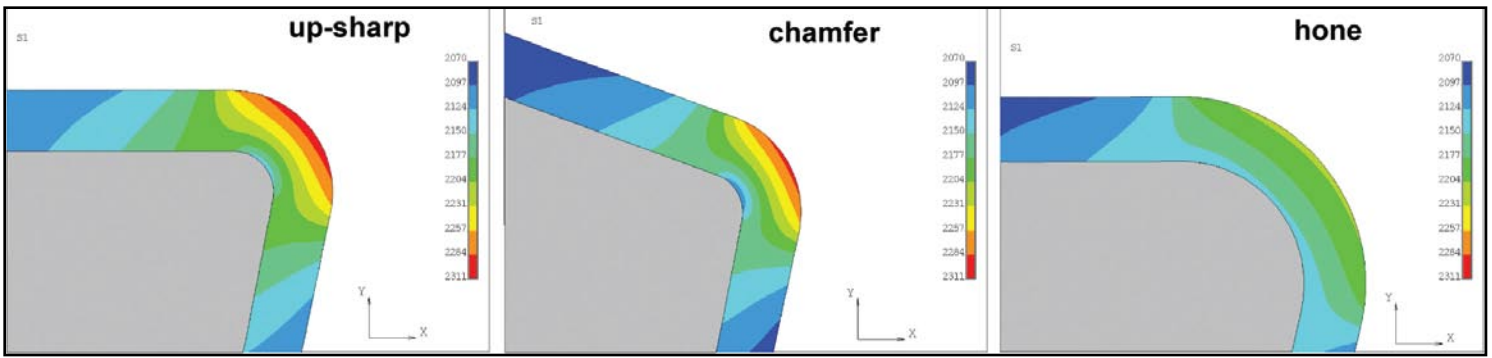


FIGURE 4: AROUND-EDGE STRESS DISTRIBUTIONS OF THREE TYPES OF EDGE PREPARATIONS MAXIMUM PRINCIPAL STRESS (MPa)

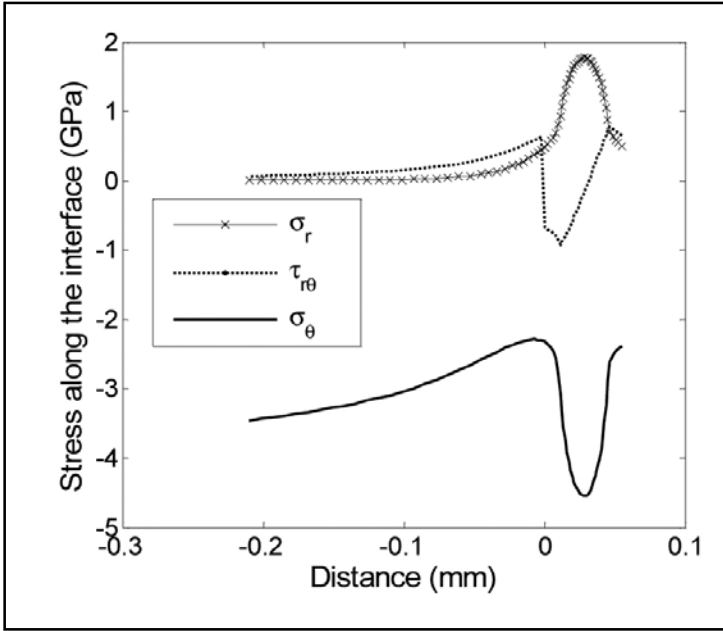


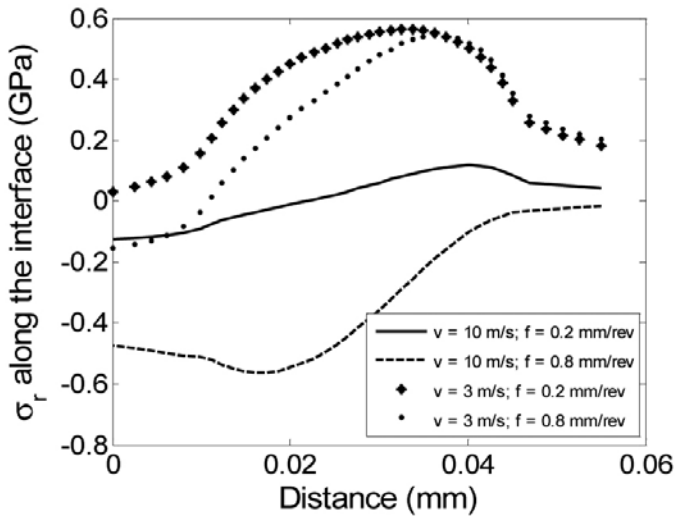
FIGURE 5: STRESS PROFILES, THREE COMPONENTS, AROUND THE CUTTING EDGE

alter considerably. The plot also shows the distortion caused by

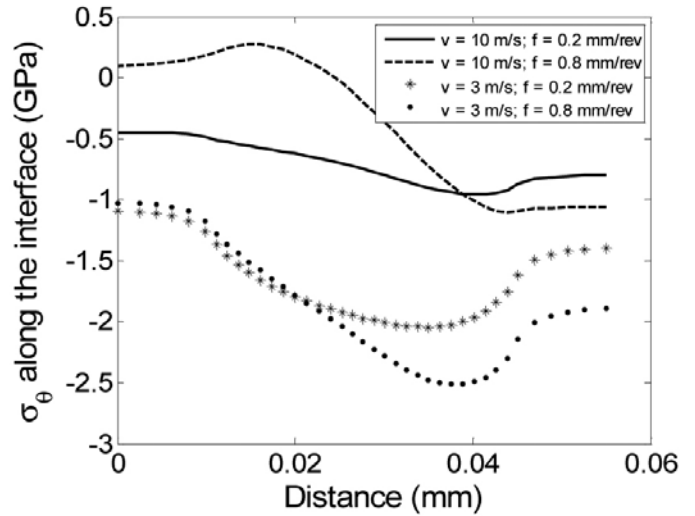
the residual stresses, about 1.7  $\mu\text{m}$  deflection in height at the center of the insert. Figure 4 compares the deposition stresses (maximum principal component) around the edge area for three different edge preparations. Clearly the edge hone (60  $\mu\text{m}$  re) has a dominant role in stress modifications and the chamfer only affects the stress concentrations at the edge slightly.

Figure 5 plots three stress components after the deposition.  $\sigma_r$  and  $\sigma_\theta$  are the normal stresses in the radial and tangential directions, and  $\tau_{\theta}$  is the shear stress in the tangential direction, respectively. The stresses are at the coating-substrate interface and plotted along the edge, also extended to the flat area (coordinate 0 is where the edge curve begins and negative values are toward away from the edge). It can be seen that at the edge, high tensile radial stresses are developed. The high tensile stresses can be detrimental in brittle fracture due to crack propagations and require greater adhesion strengths. The large compressive tangential stresses have been viewed to be beneficial for abrasive wear rate reductions, however, buckling could be another mechanism risky to the coating failure (Gahlin et al., 1996).

Figure 6 shows the deposition-stress comparisons between three different edge radii. The results clearly demonstrate that the edge radius greatly affect the stresses, both values and pattern; the maximum  $\sigma_r$  reduces from 1.8 GPa for 20  $\mu\text{m}$  re to 0.8 GPa for 100  $\mu\text{m}$  re. In addition, the large-hone case also shows smooth stress gradients along the edge. For  $\sigma_\theta$  and  $\tau_{\theta}$ , stress



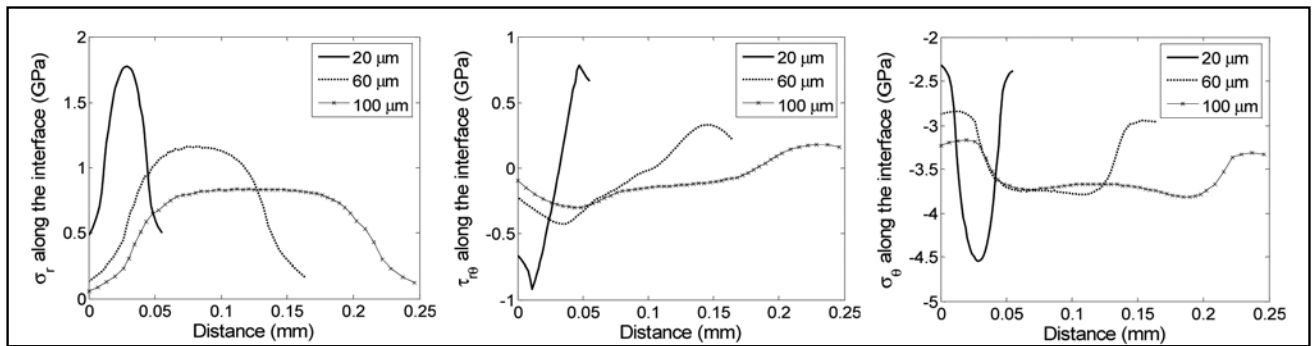
(a) Radial normal stress



(b) Tangential normal stress

FIGURE 7: MACHINING EFFECTS ON STRESS PROFILES ALONG THE INTERFACE: A) RADIAL AND B) TANGENTIAL NORMAL STRESSES

**FIGURE 6: EDGE RADIUS EFFECTS ON STRESS PROFILES AROUND THE CUTTING EDGE**



reductions at a large radius are also evident, but with a less extent in  $\tau_{r\theta}$ .

As shown above, the chamfer edge has minor effects on the deposition stress around the cutting edge, and thus, subsequent simulations with machining loading focus on only the honed edge, i.e. edge radius effects. Figures 7(a) and 7(b) show machining-parameter effects on the stress modifications,  $\sigma_r$  and  $\sigma_\theta$ , respectively, for the sharp edge case. It can be seen that the thermal and mechanical loads do strongly modify the stress distributions. The stress changes result from the combined thermal and mechanical loads in machining. Machining loading tends to reduce  $\sigma_r$  due to mechanical contact stresses. At a low cutting speed (3 m/s),  $\sigma_r$  remains mostly tensile with the high feed case slightly smaller. However, at a high cutting speed (10 m/s),  $\sigma_r$  shifts toward mostly compression with the high feed case more prominent. Thus, it can be inferred that the thermal effect is dominant. The elevated machining temperatures cause stress relief and, while balanced with the mechanical stresses, result in reduced radial stresses. For the tangential normal stress,  $\sigma_\theta$ , a similar trend is noted too, but the compression changed to tension. The machining loading tends to increase  $\sigma_\theta$ , moving toward tension. At a high speed (10 m/s), the stress relief at high machining temperatures will outweigh mechanical contact stresses (compression) and result in low compressive or even tensile stresses. At a low cutting speed (3 m/s),  $\sigma_\theta$  remains compressive, but to a less degree. A high feed keeps  $\sigma_\theta$  slightly more compressive.

The interfacial stresses have been analyzed, maximum valued compared, at different conditions: machining and assumed edge radii. Figures 8(a) and 8(b) plot  $\sigma_{\theta,max}$  and  $\sigma_{r,max}$ , respectively, affected by the edge radius with different machining parameters. It is noted that the feed seems to govern the trend of the edge

## STRESSED OUT ABOUT YOUR MOTION CONTROL SYSTEM?



**AT LEAST WHEN YOU PURCHASE AN ENCODER FROM EPC, IT WILL BE ONE LESS THING TO WORRY ABOUT.**

**PUT YOUR MIND AT EASE**

**CALL THE FRIENDLY STAFF AT EPC TODAY AND FIND OUT JUST HOW EASY IT IS TO GET THE ENCODER YOU NEED, AND FAST.**

**800-366-5412**



464276 Highway 95 South • PO Box 249 • Sagle, ID 83860  
Fax 208-263-0541 • [www.encoder.com](http://www.encoder.com) • [sales@encoder.com](mailto:sales@encoder.com)

variable indicating spline gages

Double flank gear tester

URM measurement system

FAPP fully automatic inspection & assembly systems

in-plant spline seminars

pure perfection

# FRENCO

World Leaders in Spline Gaging & Workholding and Technical Seminars

Euro-Tech Corp. 262.781.6777



Exclusive North American Distributor of:

pure perfection

**myTEC**

**FRENCO** HYDRACLAMP®

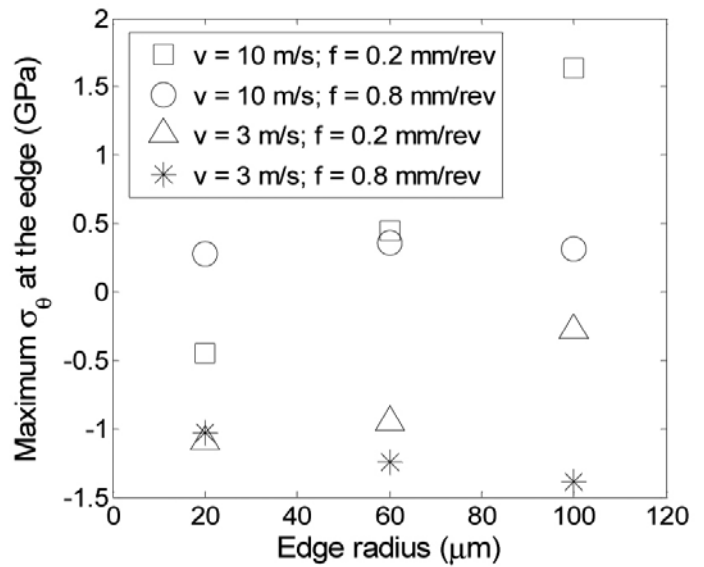
www.eurotechcorp.com

**myTEC**

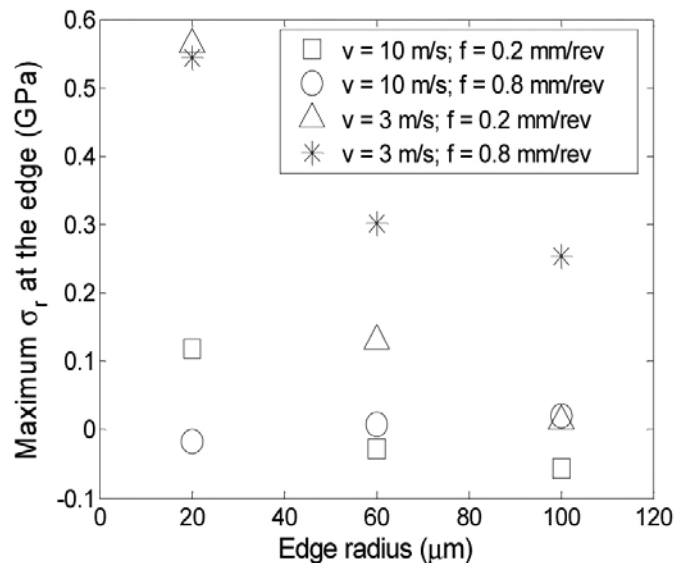
HYDRACLAMP®

HYDRAULIC -EXPANDING- CLAMPING TOOLS

- rupture proof
- incredible accuracy
- extreme holding power
- automatic or manual actuation
- no hydraulic sleeve seals



(a) Maximum tangential normal stress



(b) Maximum radial normal stress

FIGURE 8: MACHINING EFFECTS ON MAXIMUM STRESSES: A) TANGENTIAL AND B) RADIAL COMPONENTS, AS A FUNCTION OF EDGE RADIUS

radius effects. At a low feed,  $\sigma_{\theta, \text{max}}$  increases (toward tensile) with the increase of the edge radius, more evident at a high cutting speed. However, at a high feed, the edge radius has a negligible effect on  $\sigma_{\theta, \text{max}}$ , minor decreasing (more compressive) with increasing the edge radius at a low speed. Considering if compressive stresses are beneficial to wear reductions, at 10 m/s and 0.2 mm/rev, a honed edge would relatively increase tool wear compared to a sharp edge. In contrast, at 3 m/s and 0.8 mm/rev, the edge hone may be expected to slow down the tool wear. For the radial normal stress, from the simulations, large edge radii tend to shift  $\sigma_{r, \text{max}}$  toward compression except one condition, i.e. 10 m/s and 0.8 mm/rev. At 10 m/s and 0.8 mm/rev,  $\sigma_{r, \text{max}}$  increases slightly with the increase of the edge radius. Therefore, a honed edge may be considered beneficial for wear resistance.

## Conclusions

Coating delamination is the major tool failure mode of diamond coating tools, which inherits high residual stresses from the deposition process. Moreover, the stresses around the edge area are augmented due to the geometric changes and the edge radius strongly affects the deposition stresses. In addition, the cutting edge also dominates the contact stresses and heat flux conditions imposed during machining.

In this study, finite element analysis was applied to investigate edge preparation effects, in particular, the edge radius, on the deposition stresses and following stress changes due to machining. 2D thermal and mechanical analyses were conducted using linear-elastic material models for both diamond and WC. Three edge radii combined with different machining conditions (two cutting speeds and two feeds) were evaluated and stress evolutions in diamond coating tools were analyzed.

The results quantify the edge radius effects on stress concentrations around the cutting edge after the deposition.

## Appendix

(v, f)	(10,0.2)	(10,0.8)	(3,0.2)	(3,0.8)
$F_r$ (N)	46	80	70	127
$F_t$ (N)	132	432	189	495
$F_a$ (N)	52	52	91	94
$t_c$ (mm)	0.34	1.04	0.35	1.19
$l_c$ (mm)	1.03	1.51	1.73	2.23

$F_r$ : radial force,  $F_t$ : tangential force,  $F_a$ : axial force,  $t_c$ : chip thickness,  $l_c$ : tool-chip contact length.

(v, f)	(10,0.2)	(10,0.8)	(3,0.2)	(3,0.8)
$F_f$ (N)	70	95	115	158
$F_n$ (N)	132	432	189	495
$v_c$ (m/s)	5.88	7.69	1.71	2.02
q (W/mm <sup>2</sup> )	383	467	110	138
$\beta$	0.08	0.06	0.15	0.10
$\sigma$ (MPa)	123	276	106	214
$\tau$ (MPa)	65	61	64	69

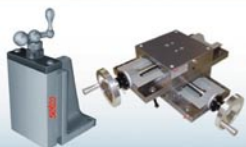
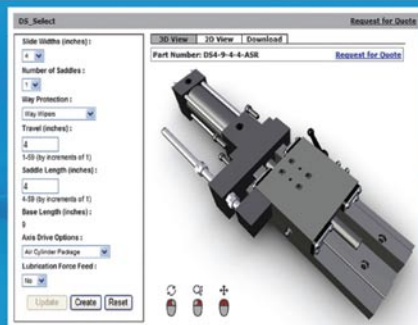
$F_f$ : frictional force,  $F_n$ : normal force,  $v_c$ : chip speed, q: rake-face heat flux ( $=F_f v_c / l_c l_w$ ),  $l_w$ : tool-chip contact width,  $\beta$ : heat partitioning coefficient,  $\sigma$ : normal stress ( $=F_n / l_c l_w$ ),  $\tau$ : shear stress ( $=F_f / l_c l_w$ ).

TABLE A1: MEASUREMENTS FROM MACHINING TESTS

TABLE A2: COMPUTED RAKE-FACE VARIABLES IN MACHINING

# THE EASY LIFE ONLINE SLIDE MODELING

Model and download ALL standard precision dovetail slide configurations from our website.



- 167 standard models
- 8 standard sizes
- Custom base and saddle lengths up to 64"
- Choice of drive styles



**setco**<sup>TM</sup>  
Set for Life

1-800-543-0470 • [setcousa.com](http://setcousa.com)  
513-941-6913 Fax • e-mail: [sales@setcousa.com](mailto:sales@setcousa.com)

© 2006 Setco Sales Co.

## When it has to be right.

- Gearbox Repair
- Gear Grinding to 94"
- Industrial Gears to 250"
- Turbo Compressor Gears
- Custom Drives
- Spline Broaching
- Gear Metrology
- Stock Planetary Speed Reducers




[www.thegearworks.com](http://www.thegearworks.com)

CUSTOM GEAR SERVICES SINCE 1946

ISO-9001

THE GEAR WORKS – SEATTLE, INC.

500 S. PORTLAND STREET • SEATTLE, WA 98108-0886  
PHONE: 206.762.3333 • FAX: 206.762.3704  
EMAIL: [SALES@THEGEARWORKS.COM](mailto:SALES@THEGEARWORKS.COM)

The radial normal stress is largely tensile and can be alleviated by a large hone; the maximum  $\sigma_r$  reduces from 1.8 GPa for 20  $\mu\text{m}$   $r_e$  to 0.8 GPa for 100  $\mu\text{m}$   $r_e$ . When the machining loading is imposed, the tangential normal stress is increased mainly due to the stress relief at elevated machining temperatures. At a high cutting speed and a high feed, the tangential normal stress,  $\sigma_{\theta, \max}$ , becomes partly tensile. For the edge radius effect, at a low feed, increasing the edge radius results in decreased  $\sigma_{\theta, \max}$  (more toward tension), which is more evident at a high cutting speed. However, at a high feed, the edge radius has a negligible effect on both  $\sigma_{\theta, \max}$  and  $\sigma_{r, \max}$ . 

***“Diamond-coated tools have great potential in various machining applications, and an advantage in the fabrication of cutting tools with complex geometry such as drills. Increased usages of lightweight high-strength components have also resulted in significant interests in diamond coating tools.”***

## Acknowledgments

This research is supported by NASA through the Alabama Space Grant Consortium. Diamond Innovations and  $\text{sp}^3$  supplied some tools. Copyright© 2007, Society of Manufacturing Engineers, SME Technical Paper TP07PUB30.

## References

- Almeida, F. A., F. J. Oliveira, M. Sousa, A. J. S. Fernandes, J. Sacramento, and R. F. Silva, (2005), “Machining hardmetal with CVD diamond direct coated ceramic tools: effect of tool edge geometry,” *Diamond and Related Materials*, Vol. 14(3-7), pp. 651-656.
- Amirhaghi, S., H. S. Reehal, R. J. K. Wood, and D. W. Wheeler, (2001), “Diamond coatings on tungsten carbide and their erosive wear properties,” *Surface and Coatings Technology*, Vol. 135, pp. 126-138.
- Arumugam, P. U., A. P. Malshe, and S. A. Batzer, (2006), “Dry machining of aluminum–silicon alloy using polished CVD diamond coated cutting tools inserts,” *Surface and Coatings Technology*, Vol. 200(11), pp. 3399-3403.
- Catledge, S. A. and Y. K. Vohra, (1995), “High density plasma processing of diamond films on titanium: Residual stress and adhesion measurements,” *Journal of Applied Physics*, Vol. 78(12), pp. 7053-7058.
- Chou, Y. K. and J. Liu, (2005), “CVD Diamond Tool Performance in Composite Machining,” *Surface and Coatings Technology*, Vol. 200, pp. 1872-1878.
- Davim, J. P., (2002), “Diamond tool performance in machining metal–matrix composites,” *Journal of Materials Processing Technology*, Vol. 128(1-3), pp. 100-105.
- D’Errico, G. E., and R. Calzavarini, (2001), “Turning of metal matrix composites,” *Journal of Materials Processing Technology*, Vol. 119(1-3), pp. 257-260.
- Gahlin, R., A. Alahelisten, and S. Jacobson, (1996), “The effects of compressive stresses on the abrasion of diamond coatings,” *Wear*, Vol. 196(1-2), pp. 226-233.
- Gunnars, J., and A. Alahelisten, (1996), “Thermal stresses in diamond coatings and their influence on coating wear and failure,” *Surface and Coatings Technology*, Vol. 80(3), pp. 303-312.
- Heath, P. J., (1986), “Properties and Uses of Amorphite,” *Industrial Diamond Review*, Vol. 46, pp. 120-127.
- Hu, J., Y. K. Chou, and R. G. Thompson, (2007), “Characterization of nanocrystalline diamond coating cutting tools,” *International Conference on Metallurgical Coatings and Thin Films*, San Diego, CA, April 23 – 27, 2007, accepted for publication.
- Karner, J., M. Pedrazzini, I. Reineck, M. E. Sjöstrand, and E. Bergmann, (1996), “CVD diamond coated cemented carbide cutting tools,” *Materials Science and Engineering A*, Vol. 209(1-2), pp. 405-413.
- Liu, J. and Y. K. Chou, (2005), “An Investigation on Cutting Tool Temperatures in Composite Machining Assisted with Heat-pipe Cooling,” *Proceedings of ASME IMECE, Manufacturing Science and Engineering*, Orlando, Florida, Nov. 6-11, IMECE2005-80323 (in CD).
- Mallika, K. and R. Komanduri, (1999), “Diamond coatings on cemented tungsten carbide tools by low-pressure microwave CVD,” *Wear*, Vol. 224(2), pp. 245-266.
- Oles, E. J., A. Inspektor, and C. E. Bauer, (1996), “The new diamond-coated carbide cutting tools,” *Diamond and Related Materials*, Vol. 5(6-8), pp. 617-624.
- Polini, R., F. Casadei, P. D’Antonio, and E. Traversa, (2003), “Dry turning of alumina/aluminum composites with CVD diamond coated Co-cemented tungsten carbide tools,” *Surface and Coatings Technology*, Vol. 166(2-3), pp. 127-134.
- Schafer, L., M. Fryda, T. Stolley, L. Xiang, and C.-P. Klages, (1999), “Chemical vapour deposition of polycrystalline diamond films on high-speed steel,” *Surface and Coatings Technology*, Vol. 116-119, pp. 447-451.
- Shen, C. H., (1994), “Machining Performance of Thin Film Diamond Coated Inserts on 390 Aluminum,” *Transactions of the North American Manufacturing Research Institution of SME*, Vol. 22, pp. 201-208.
- Shen, C. H., (1996), “The importance of diamond coated tools for agile manufacturing and dry machining,” *Surface and Coatings Technology*, Vol. 86-87(2), pp. 672-677.
- Thiele, J. D. and S. N. Melkote, (1999), “Effect of cutting edge geometry and workpiece hardness on surface generation in the finish hard turning of AISI 52100 steel,” *Journal of Materials Processing Technology*, Vol. 94, pp. 216-226.

## ABOUT THE AUTHORS:

Jianwen Hu and Y. Kevin Chou are with the Department of Mechanical Engineering at the University of Alabama in Tuscaloosa. Go to [me.eng.ua.edu]. Raymond G. Thompson is with Vista Engineering, Inc. [www.vistaeng.com].